

# The effects of solvents on the formation of sol–gel-derived $\text{Bi}_{12}\text{SiO}_{20}$ thin films

Asja Veber<sup>a,\*</sup>, Špela Kunej<sup>a</sup>, Romana Cerc Korošec<sup>b</sup>, Danilo Suvorov<sup>a</sup>

<sup>a</sup> Advanced Materials Department, Jožef Stefan Institute, Jamova 39, 1001 Ljubljana, Slovenia

<sup>b</sup> Faculty of Chemistry and Chemical Technology, University of Ljubljana, Aškerčeva 5, 1000 Ljubljana, Slovenia

Received 23 October 2009; received in revised form 20 April 2010; accepted 23 April 2010

Available online 18 May 2010

## Abstract

The sol–gel method was used to synthesize  $\text{Bi}_{12}\text{SiO}_{20}$  thin films. Two synthesis routes with two different solvents, i.e., 2-ethoxyethanol and acetic acid, were used and compared. Thin films were deposited onto Pt/TiO<sub>2</sub>/SiO<sub>2</sub>/Si substrates by spin-coating at 3000 rpm and annealed at 700 °C for 1 h. A different coordination of the bismuth ion was observed in the sols prepared with acetic acid (AcOH), and as a result, stable sols were formed with a shorter gelation time  $t_G = 84$  h ( $c = 0.76$  M), when compared with the sols prepared from 2-ethoxyethanol (EtoEtOH)  $t_G = 580$  h ( $c = 0.76$  M). The microstructures of the  $\text{Bi}_{12}\text{SiO}_{20}$  thin films prepared from sols using EtoEtOH were homogeneous and dense. On the other hand, a porous microstructure was observed for the  $\text{Bi}_{12}\text{SiO}_{20}$  thin films deposited from the sol in which AcOH was used as the solvent.

© 2010 Elsevier Ltd. All rights reserved.

**Keywords:** Sol–gel process; Thin film;  $\text{Bi}_{12}\text{SiO}_{20}$

## 1. Introduction

Bismuth oxide ( $\text{Bi}_2\text{O}_3$ ) exhibits a rich phase polymorphism. It is known to exist in the  $\alpha$ -monoclinic,  $\beta$ -tetragonal,  $\gamma$ -body-centered (bcc), and  $\delta$ -face-centered cubic (fcc) structures. The stable or metastable occurrence of these phases depends on the various temperature/thermal treatment conditions and chemical doping.<sup>1</sup> Among them, the  $\gamma$ -bcc phase has been of particular interest, at both the fundamental and technological levels. The body-centered-cubic  $\gamma$ -form of pure  $\text{Bi}_2\text{O}_3$  is a metastable compound, which forms during the cooling of the high-temperature-stable fcc  $\delta$ -phase.<sup>1</sup> The  $\gamma$ -phase can be stabilized by the addition of a small amount of other cations, such as Si, Ge, Ti, Ga, etc., forming the  $\text{Bi}_{12}\text{MO}_{20}$ -type compound,<sup>2</sup> where M represents the doping cations. Raadaev and Simonov<sup>3</sup> confirmed that in such a compound the Bi atoms also enter the B-sites of the structure and a new general formula was proposed:  $\text{Bi}_{12}(\text{Bi}_{4/5-nx}\text{M}_{5x}^{n+})\text{O}_{19.2+nx}$  ( $0 \leq x \leq 0.2$ ). Among the various sillenite compounds described in the literature, the only stoichiometric compound is  $\text{Bi}_{12}\text{SiO}_{20}$ .<sup>4</sup> This  $\text{Bi}_{12}\text{SiO}_{20}$  material has

been investigated as a useful dielectric for electronic devices. The microwave dielectric properties of  $\text{Bi}_{12}\text{SiO}_{20}$  (5.5 GHz:  $\varepsilon_r = 40$ ,  $\tau_f = 20$  ppm/K and  $Q \times f = 8100$  GHz) prepared by solid-state reaction were reported by Valant and Suvorov.<sup>5</sup>

New applications and the recent miniaturization of electronic devices have resulted in a constant drive to produce a thinner dielectric layer, and therefore a lot of attention has been focused on the preparation of dielectric thin films.<sup>6–10</sup> Among the various methods of thin film synthesis, the sol–gel method offers an attractive route for the fabrication of such electronic devices.

Sol–gel chemistry is based on inorganic polymerization reactions, which allow the synthesis of ceramic materials with a high degree of homogeneity. This is due to the mixing of the metallic precursors at the molecular level in the solution. The polymerization starts with the hydroxylation of the alkoxide precursors through the hydrolysis of the alkoxo group; this is then followed by the polycondensation reaction (oxolation, olation). These reactions, i.e., hydrolysis, oxolation and olation, are involved in the transformation of a molecular alkoxide precursor into an oxide network. Chemical additives, for example, solvents, stabilizing agents or drying-control chemical additives, are normally used to improve the sol–gel process. Sol gels can be synthesized with a wide range of different solvents. These solvents behave as true chemical reagents, and as such are able to react with

\* Corresponding author.

E-mail address: [asja.veber@ijs.si](mailto:asja.veber@ijs.si) (A. Veber).

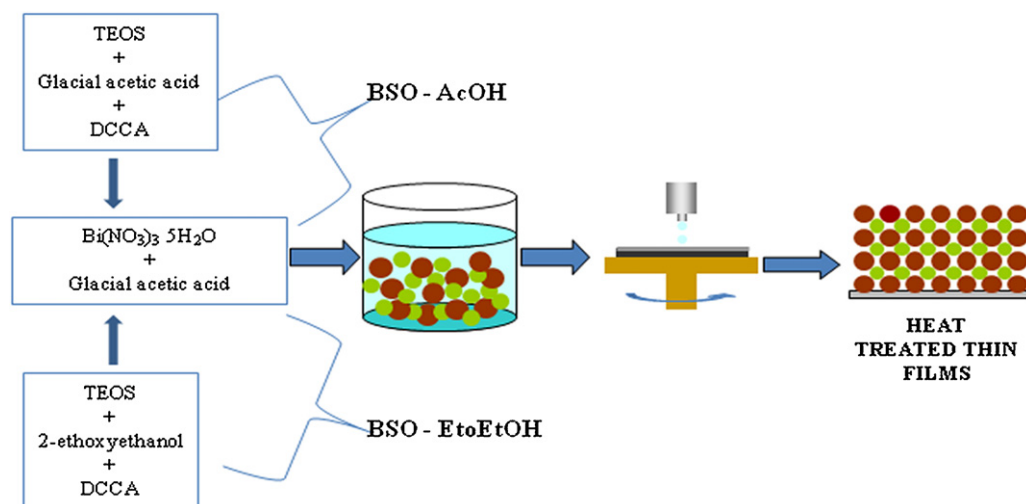


Fig. 1. The synthesis procedures for the BSO thin films.

the precursors<sup>11</sup> and thus change them at the molecular level, so altering the whole sol–gel process. The key aspect of this process is the chemical stability of the sol, which directly determines the properties of the thin films that are formed.

There are only a few reports available in the literature on the synthesis of  $\text{Bi}_{12}\text{SiO}_{20}$  thin films using the sol–gel method,<sup>12,13</sup> and no systematic study of the solvent's influence on the chemical stability of the sols and the microstructural development of BSO thin films has been reported, yet. Based on previous experiments, however, one would expect that the solvent has an important contribution to the microstructural development and consequently on the final dielectric properties of the thin film. We found that the preparation of BSO thin films deposited from sols using bismuth nitrate as a precursor is very complex due to the re-crystallization of the bismuth nitrate, which results in unstable sols. Therefore, our experiments were focused on a detailed study of the chemical stability of the sols produced with the use of two different solvents. In addition, we examined the chemical reactions that occur in the sol–gel process using FT-IR spectroscopy. The BSO phase formation was determined with XRD, and the microstructural development was studied with AFM and SEM.

## 2. Experimental

For the deposition of the BSO thin films, the sols were prepared using  $\text{Bi}(\text{NO}_3)_3 \cdot 5\text{H}_2\text{O}$  (Alfa Aesar, 98%) and  $\text{Si}(\text{OC}_2\text{H}_5)_4$  (TEOS) (Alfa Aesar, 98%) as the precursors, 2-ethoxyethanol (EtoEtOH) (Alfa Aesar, 99%) and glacial acetic acid (AcOH) (Alfa Aesar, 99.7+%) as the solvents, and formamid (Alfa Aesar, 99%) as the drying-control chemical additive. The sols were prepared with two procedures: using 2-ethoxyethanol as the co-solvent, referred to as BSO-EtoEtOH; or using acetic acid as the co-solvent, referred to as BSO-AcOH. Fig. 1 shows the two synthesis procedures for the BSO thin films.

First, the  $\text{Bi}(\text{NO}_3)_3 \cdot 5\text{H}_2\text{O}$  was dissolved in the acetic acid at a temperature of 40 °C. Next, the TEOS was mixed with 2-ethoxyethanol or acetic acid. The final step was mixing together

the solution of bismuth salt and the solution of TEOS, forming the sols BSO-EtoEtOH or BSO-AcOH. Formamide was added to control the rate of the polymerization. Sols with a concentration from 0.55 to 1.2 M were filtered through 0.2- $\mu\text{m}$  filters and deposited onto the Pt/TiO<sub>2</sub>/SiO<sub>2</sub>/Si substrate using the spin-coating method at 3000 rpm for 30 s. The thin film consisted of four layers. Each layer was heated on a hot-plate for 2 min at 250 °C to pyrolyze the organic compounds before the deposition of the next layer. The thin films were annealed in the temperature range from 300 to 700 °C for 1 h.

Infrared spectroscopy (FT-IR) (IFS 66/S, Bruker) was used to analyze the reaction mechanisms involved in the sol–gel process; thermal analysis (TG), evolved-gas analysis (EGA) (Netzsch STA 449C) and differential scanning calorimetry (DSC) (Mettler Toledo DSC 822e) were used to determine the pre-heating temperature of the thin films; and X-ray diffraction (XRD) (D4, ENDEAVOR, Bruker Axs) was used to determine the phases appearing in the thin films. The microstructure development of the films was investigated with scanning electron microscopy (SEM) (SUPRA 35 VP, Carl Zeiss) and atomic force microscopy (AFM) (VEECO DIMENSION 3100).

## 3. Results and discussion

### 3.1. Reaction mechanism in the sol–gel process

For a better understanding of the basic reactions involved in the BSO-AcOH and BSO-EtoEtOH sols, an extensive study was carried out using infrared (FT-IR) spectroscopy.

Fig. 2 shows the FT-IR spectra for dried amorphous thin films deposited on Si substrates from the sols: (curve a) BSO-AcOH and (curve b) BSO-EtoEtOH.

The IR spectra of the thermally untreated thin film deposited from the BSO-AcOH sol (Fig. 2, curve a) exhibits bands located at 1670 and 1288  $\text{cm}^{-1}$ , which are ascribed to the asymmetric and symmetric vibrations of the C=O groups bonded to the organic ( $-\text{CH}_3$ ) groups and monodentately coordinated to the

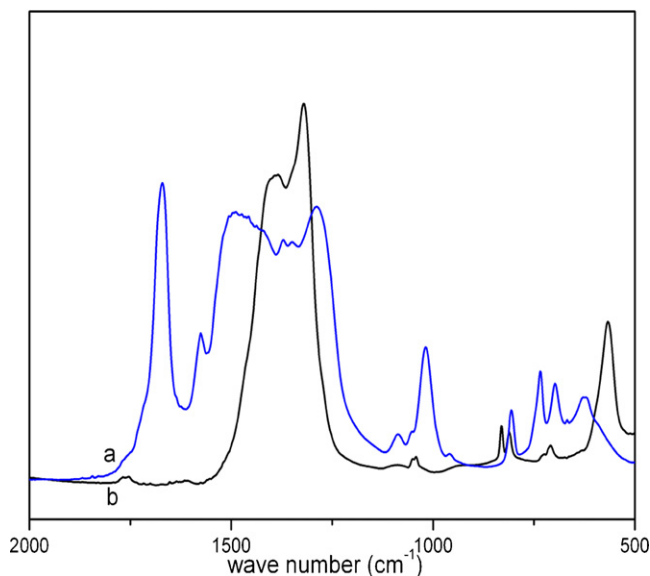


Fig. 2. The IR spectra of the sols: (curve a) BSO-AcOH and (curve b) BSO-EtOH.

bismuth. The bands at  $1575$  and  $1490\text{ cm}^{-1}$  are attributed to the asymmetric ( $\nu_a(\text{COO}^-)$ ) and symmetric ( $\nu_s(\text{COO}^-)$ ) vibrations of the carboxylate groups, which are bidentately coordinated to the bismuth ion. The absorption band centered at  $1087\text{ cm}^{-1}$  was attributed to the Si–O–Si asymmetric stretching vibration. The bands located at  $1018$ ,  $697$  and  $621\text{ cm}^{-1}$  were associated with the vibration of carboxylate groups bonded to the bismuth ion. The bands at  $805$  and  $734\text{ cm}^{-1}$  were related to the vibration of the N–O out-of-plane and in-plane bands.

Fig. 2 (curve b) shows the infrared spectrum for the as-deposited thin film from the BSO-EtOH sol. The absorption bands located at  $1384$ ,  $830$ ,  $811$  and  $710\text{ cm}^{-1}$  were assigned to the vibrations of the N–O stretch. The bands at  $1755$  and  $1320\text{ cm}^{-1}$  are attributed to the stretching vibration of the carboxylate group. The band at  $1086\text{ cm}^{-1}$  was related to the asymmetric stretch of the Si–O–Si bond. The band located at  $566\text{ cm}^{-1}$  was assigned to the vibration of the Bi–O bond. In the thin films deposited from the BSO-EtOH sol the bismuth ions are coordinated by nitrate ligands.

A comparison of the FT-IR spectra of thin films deposited from sols BSO-AcOH (Fig. 2, curve a) and BSO-EtOH (Fig. 2, curve b) clearly indicates the differences in the bismuth coordination sphere. It was found that in the thin film deposited from the BSO-AcOH sol the bismuth is coordinated by carboxylate ligands, while in thin films deposited from the BSO-EtOH sol the bismuth is coordinated by nitrate ligands. It is well known that the reaction mechanism of gel formation is influenced by the coordination sphere of the precursor.<sup>14</sup> In the thin film deposited from the BSO-AcOH sol carboxylate ligands that coordinate the bismuth ion cause its oligomerization. Therefore, the gel forms by the incorporation of the silicon network with the bismuth network. In contrast, in thin films deposited from the BSO-EtOH sol, where the nitrate ligands coordinate the bismuth ion, oligomerization does not occur.<sup>15</sup> Therefore, the gel forms by the entrapment of bismuth ions in the silica network.

### 3.2. Influence of the solvent on the gelation time of the sols

The influence of the solvent on the stability and the gelation time of the BSO-AcOH and BSO-EtOH sols is shown in Fig. 3. The gelation times for the BSO-AcOH sols (Fig. 3(a)) were shorter than for the equivalent 2-ethoxyethanol solutions (Fig. 3(b)) due to the catalytic effect of the acetic acid. In the BSO-EtOH sols the 2-ethoxyethanol reacts with the acetic acid, thereby reducing its catalytic effect by forming an ester, and so decreasing the reaction rate of the hydrolysis and condensation. For a concentration of  $0.76\text{ M}$  for the BSO-EtOH sol, the time of gelation was  $580\text{ h}$ . However, when the BSO-AcOH sol was used the gelation time was found to be a significantly shorter  $84\text{ h}$ .

In the BSO-AcOH sols, no precipitation of the bismuth salt occurred due to the reaction between the acetic acid and the bismuth salt. The bismuth ions, monodentately and bidentately coordinated with carboxylate ligands, were no longer prone to re-crystallization, while in the BSO-EtOH sols, where the bismuth ions are coordinated with nitrate ligands, the precipitation occurs below a concentration of  $0.76\text{ M}$ . According to an earlier reported study,<sup>16</sup> the precipitation occurred due to the hydrolysis of the bismuth salt.

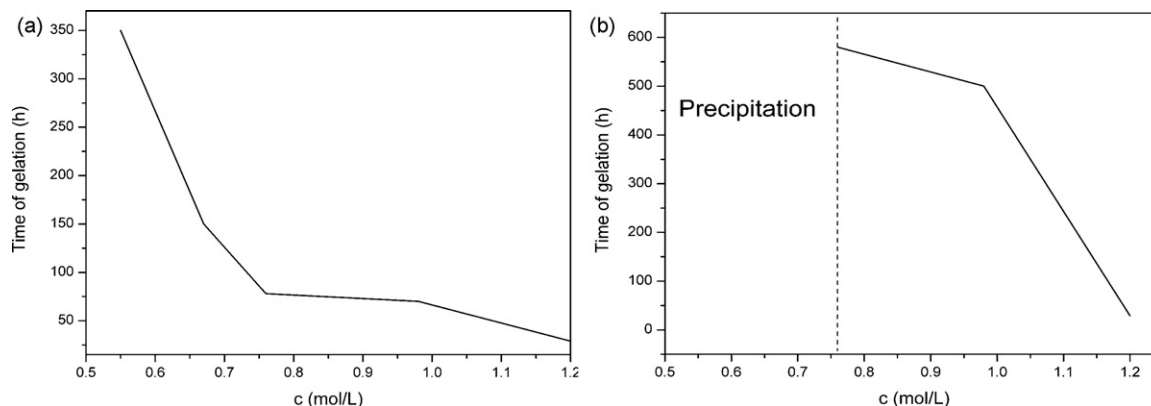


Fig. 3. Stability of the sols: (a) BSO-AcOH and (b) BSO-EtOH.

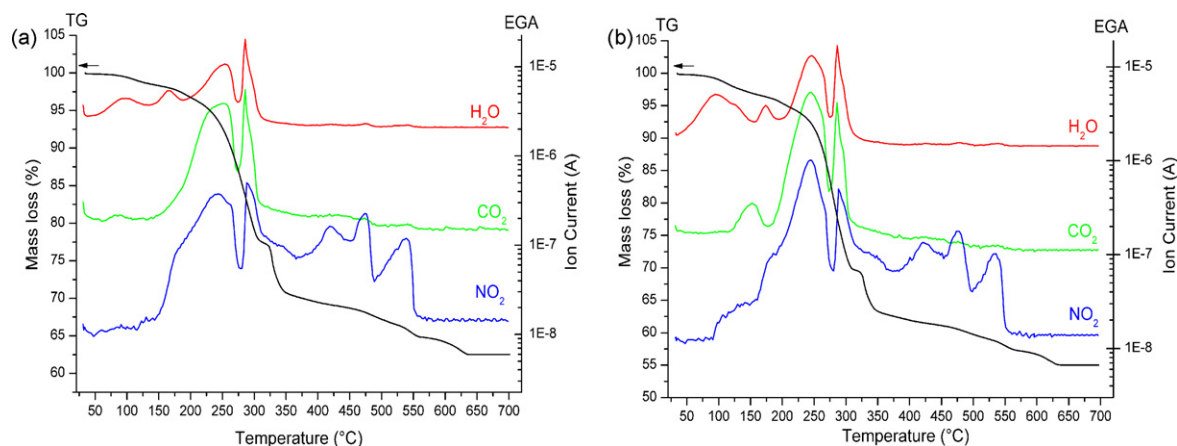


Fig. 4. TG/EGA analyses of the xerogel: (a) S-AcOH and (b) S-EtoEtOH.

### 3.3. Film characterization

An important parameter for the preparation of a dense thin film is to determine the pre-heating temperature of the thin film after the deposition. During the pre-heating of the thin films, two mechanisms are present, i.e., gelation and solvent evaporation. If the pre-heating temperature is too low, the gelation occurs more rapidly than the solvent evaporation. This leads to the entrapment of the solvent in the gel network, which during annealing causes the formation of a porous microstructure. In contrast, if the pre-heating temperature is too high the stress caused by the rapid volatilization of the solvent and the decomposition of the gel then results in the peeling of the thin film from the substrate.

To determine the pre-heating temperature of the thin films after the spin-coating deposition, TG/EGA analyses were performed on the BSO-AcOH and BSO-EtoEtOH sols in air, as shown in Fig. 4. It is clear that the BSO-AcOH (Fig. 4(a)) and BSO-EtoEtOH (Fig. 4(b)) xerogels exhibit similar decomposition behaviours.

In the TG curves a large decrease in weight from 100 to 300 °C was observed. The EGA curves for both xerogels showed that in the temperature range between 100 and 300 °C the mass peaks correspond to the evaporation of water, the nitrate groups

and the decomposed organic compounds. In the temperature range between 300 and 550 °C, only the evaporation of a nitrate group took place.

The TG and DSC curves of the thin film deposited from the BSO-EtoEtOH sol is shown in Fig. 5. A large decrease in the weight was observed in the temperature range between 100 and 250 °C accompanying with a sharp exothermic peak due to the thermal decomposition of the nitrates and the organic matter. Similar results were obtained in the thin film deposited from the BSO-AcOH sol.

For the thin film the most intensive decomposition occurs at a lower temperature (250 °C) than for the amorphous xerogel (300 °C). It is known that thermally induced processes in the thin film samples occur at lower temperatures with regard to the xerogel due to the smaller sample size.<sup>17</sup> Therefore, the pre-heating temperature for the preparation of BSO thin films was determined to be 250 °C. Using a pre-heating temperature above 250 °C resulted in the peeling of the BSO thin film from the substrate.

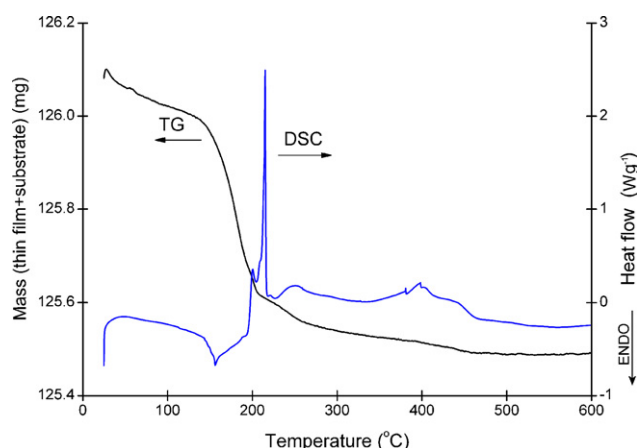


Fig. 5. TG analysis of the thin film deposited from the S-EtoEtOH sol.

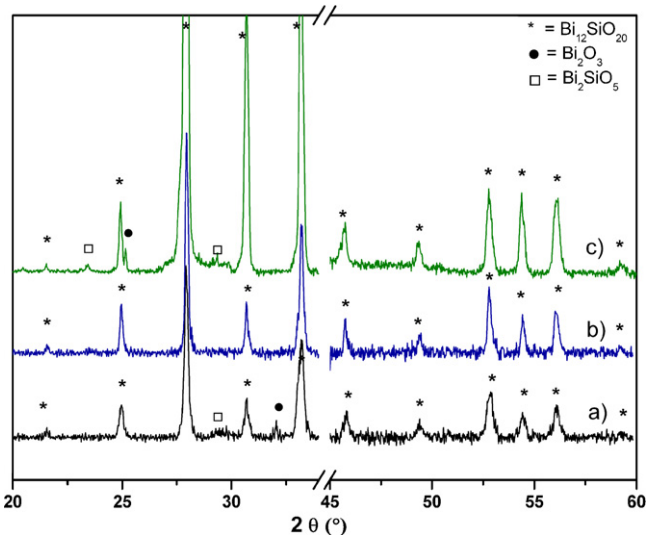


Fig. 6. XRD patterns of the BSO thin films annealed at temperature: (curve a) 600 °C, (curve b) 700 °C deposited from BSO-EtoEtOH sol and (curve c) 700 °C deposited from BSO-AcOH sol.



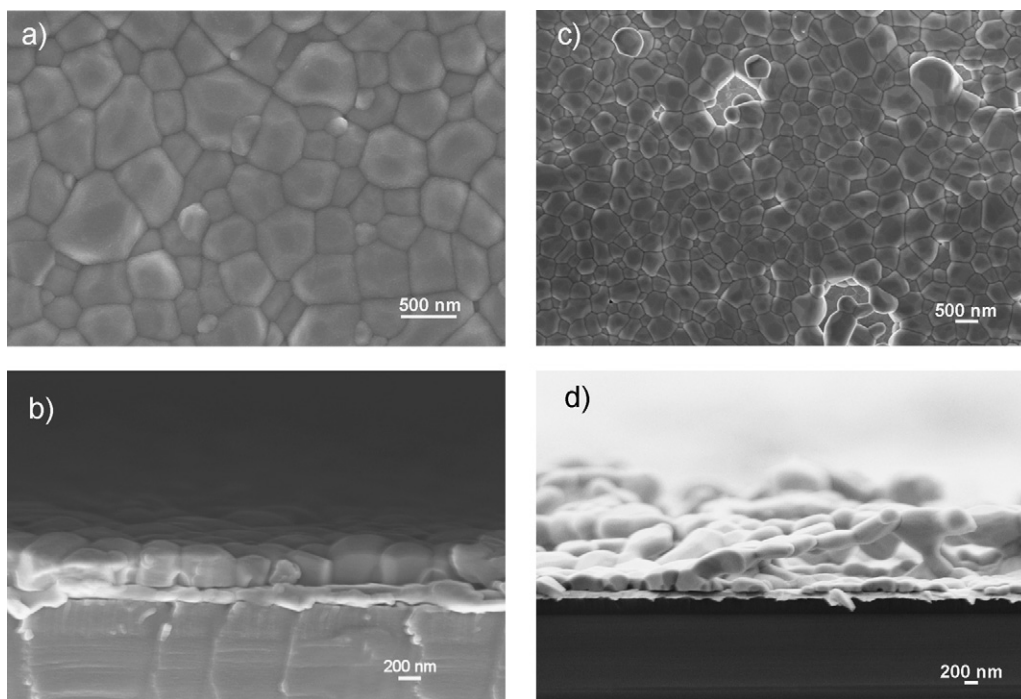


Fig. 7. Micrographs of the (a) microstructure, (b) cross-section of BSO thin films deposited from sol BSO-EtOEtOH and (c) microstructure, (d) cross-section of BSO thin films deposited from sol BSO-AcOH.

In order to determine the formation of the single BSO phase, XRD analyses were performed on thin films deposited from the BSO-AcOH and BSO-EtOEtOH sols that were annealed at temperatures of 600 and 700 °C (Fig. 6). At 600 °C the majority of the reflections belong to the sillenite BSO phase; however, there are still traces of the bismuth oxide and  $\text{Bi}_2\text{SiO}_5$  phases present. When the annealing temperature was increased to 700 °C for the thin film deposited from the BSO-EtOEtOH sol the only detected phase was BSO. In contrast, in the thin films prepared from the BSO-AcOH sol, secondary phases of  $\text{Bi}_2\text{O}_3$  and  $\text{Bi}_2\text{SiO}_5$  were still detected.

Fig. 7(a) and (b) show the microstructure development and cross-section of the BSO thin films deposited from the

BSO-EtOEtOH. The BSO thin film resulted in a dense and homogeneous microstructure with a thickness of 250 nm. In contrast, thin films deposited from the BSO-AcOH sol (Fig. 7(c) and (d)) showed a non-uniform microstructure with an approximate thickness of 300 nm. The microstructure of the BSO (Fig. 7(c) and (d)) indicates that the thin film becomes a gel before it dries. This means that a lot of solvent was trapped in the thin film during the evaporation and the heat-treatment processes, which resulted in a high porosity.

The roughness measured by AFM ranged from 60 to 500 nm for the BSO thin films prepared from the BSO-AcOH sol (Fig. 8(b)), while the roughness of the BSO thin films prepared from the BSO-EtOEtOH sol was 30 nm (Fig. 8(a)).

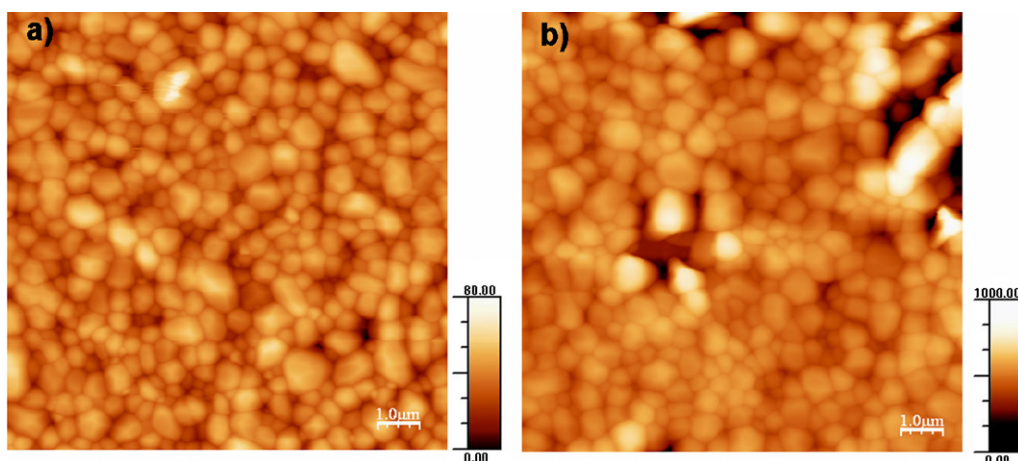


Fig. 8. Images of the morphology of BSO thin films deposited from sols: (a) BSO-EtOEtOH and (b) BSO-AcOH.

#### 4. Conclusions

BSO thin films were deposited from different sols and annealed at 700 °C. We observed that the co-solvent had a significant influence on the stability of the sols and the quality of the BSO thin films. By comparing the reaction mechanism of the BSO-EtOH and BSO-AcOH sols we were able to conclude that the hydrolysis and condensation reactions are more pronounced in the BSO-AcOH sol, which results in a shorter gelation time ( $c = 0.76$  M,  $t_G = 84$  h) compared to the BSO-EtOH sol ( $c = 0.76$  M,  $t_G = 580$  h). The reaction between the bismuth ion and the acetic acid resulted in the formation of monodentate and bidentate chelates, which prevented the precipitation of bismuth nitrate. We found that the same pre-heating temperature of 250 °C can be used for the deposition of BSO thin films from the sols BSO-EtOH and BSO-AcOH. The deposition of the BSO thin films on Si/SiO<sub>2</sub>/TiO<sub>2</sub>/Pt from the BSO-EtOH sol resulted in a homogeneous and dense microstructure with a thickness of 250 nm, while the BSO thin films deposited from the S-AcOH sol resulted in a porous and non-uniform microstructure with an approximate thickness of 300 nm.

#### Acknowledgement

We thank B. Orel of the National Institute of Chemistry, Slovenia, for fruitful discussions.

#### References

1. Chehab S, Conflant P, Drache M, Boivin JC, McDonald G. Solid-state reaction pathways of sillenite-phase formation studied by high-temperature X-ray diffractometry and differential thermal analysis. *Mater Res Bull* 2003;**38**:875–97.
2. Fu S, Ozoe H. Reaction pathways in the synthesis of photorefractive  $\gamma$ -Bi<sub>12</sub>MO<sub>20</sub> (M = Si, Ge, or Ti). *J Am Ceram Soc* 1997;**80**:2501–9.
3. Radaev SF, Simonov VI. Structure of sillenites and atomic mechanisms of their isomorphic substitutions. *Sov Phys Crystallogr (Engl Transl)* 1992;**37**:484–99.
4. Valant M, Suvorov D. A Stoichiometric model for sillenites. *Chem Mater* 2002;**14**:3471–6.
5. Valant M, Suvorov D. Processing and dielectric properties of sillenite compounds Bi<sub>12</sub>MO<sub>20-δ</sub> (M = Si, Ge, Ti, Pb, Mn, B<sub>1/2</sub>P<sub>1/2</sub>). *J Am Ceram Soc* 2001;**84**:2900–4.
6. Madeswaran S, Giridharan NV, Jayavel R. Sol–gel synthesis and property studies of layered perovskite bismuth titanate thin films. *Mater Chem Phys* 2003;**80**:23–8.
7. Song S, Zhai J, Yao X. Effects of buffer layer on the dielectric properties of BaTiO<sub>3</sub> thin films prepared by sol–gel method. *Mater Sci Eng B* 2007;**145**:28–33.
8. Kong LB, Ma J. Randomly oriented Bi<sub>4</sub>Ti<sub>3</sub>O<sub>12</sub> thin films derived from a sol–gel process. *Thin Solid Films* 2000;**379**:89–93.
9. Fuierer P, Li B. Nonepitaxial orientation in sol–gel bismuth titanate films. *J Am Ceram Soc* 2002;**85**:299–3048.
10. Adikory SU, Chan HLW. Ferroelectric and dielectric properties of sol–gel derived Ba<sub>x</sub>Sr<sub>1-x</sub>TiO<sub>3</sub>. *Thin Solid Films* 2003;**424**:70–4.
11. Fidalgo A, Ilharco LM. Thickness and structure of sol–gel hybrid films. II. The role of the solvent. *J Sol–Gel Sci* 2003;**26**:357–436.
12. Klebanski EO, Kudzin AY, Pasaľ'Ski VM, Plyaka SN, Sadovskaya Lya, Sokolyanski GKh. Thin sol–gel bismuth silicate films. *Phys Solid State* 1999;**41**:913–5.
13. Plyaka SN, Sokolyanskii GCh, Klebanski EO. Conductivity of the Bi<sub>12</sub>SiO<sub>20</sub> thin films. *Condens Matter Phys* 1999;**2**:625–30.
14. Brinker CJ, Scherer GW. *Sol–gel science: the physics and chemistry of sol–gel processing*. New York: Academic Press; 1989.
15. Bachman RE, Whitmire KH, Thurston JH, Gulea A, Stavila O, Stavila V. Bismuth ladder polymers: structural and thermal studies of [Bi(OCH<sub>2</sub>CH<sub>2</sub>)<sub>3</sub>N]<sub>n</sub> and [Bi<sub>x</sub>Tb<sub>1-x</sub>(O<sub>2</sub>C<sub>2</sub>H<sub>2</sub>)<sub>3</sub>N·2H<sub>2</sub>O]<sub>n</sub>. *Inorg Chim Acta* 2003;**346**:249–55.
16. Gu H, Dong C, Chen P, Bao D, Kuang A, Li X. Growth of layered perovskite Bi<sub>4</sub>Ti<sub>3</sub>O<sub>12</sub> thin films by sol–gel method. *J Cryst Growth* 1998;**186**:403–8.
17. Cerc Korošec R, Bukovec P. Sol–gel prepared NiO thin films for electrochromic applications. *Acta Chim Slov* 2006;**53**:136–47.